# Directional Bilateral Asymmetry in Fish Otolith: A Potential Tool to Evaluate Stock Boundaries?

Kelig Mahe, Kirsteen Mackenzie, Djamila Ider, Andrea Massaro, Oussama Hamed, Alba Jurado-Ruzafa, Patricia Goncalves, Aikaterini Anastasopoulou, Angelique Jadaud, Chryssi Mytilineou, et al.

symmetry

MDPI

*Article*

# Directional Bilateral Asymmetry in Fish Otolith: A Potential Tool to Evaluate Stock Boundaries?

**Kélig Mahé [1,*], Kirsteen MacKenzie [1], Djamila Ider [2,3], Andrea Massaro [4], Oussama Hamed [5], Alba Jurado-Ruzafa [6], Patrícia Gonçalves [7], Aikaterini Anastasopoulou [8], Angelique Jadaud [9], Chryssi Mytilineou [8], Marine Randon [10], Romain Elleboode [1], Alaia Morell [1], Zouhir Ramdane [2], Joanne Smith [11], Karen Bekaert [12], Rachid Amara [13], Hélène de Pontual [14] and Bruno Ernande [15,16]**

1 IFREMER, Fisheries Laboratory, 150 quai Gambetta, BP 699, 62200 Boulogne-sur-mer, France; kirsteen.mackenzie@ifremer.fr (K.M.); romain.elleboode@ifremer.fr (R.E.); Alaia.Morell@ifremer.fr (A.M.)
2 Laboratoire de Zoologie Appliquée et d'Ecophysiologie Animale, Université Abderrahmane Mira, Béjaïa 06000, Algeria; dj.ider@univ-bouira.dz (D.I.); zouhir.ramdane@univ-bejaia.dz (Z.R.)
3 Faculté des Sciences de la Nature et de la Vie et des Sciences de la Terre, Université de Bouira, Bouira 10000, Algeria
4 APLYSIA—Via Menichetti 35, 27121 Livorno, Italy; andrea.massaro@aplysia.it
5 Campus Universitaire, Université de Tunis El Manar, El Manar II 2092, Tunisia; hamed.o@opaliarecordati.com
6 Centro Oceanográfico de Canarias, Instituto Español de Oceanografía (IEO, CSIC), 38180 Santa Cruz de Tenerife, Spain; alba.jurado@ieo.es
7 Departamento do Mar e dos Recursos Marinhos, Instituto Português do Mar e da Atmosfera (IPMA), 1495-006 Lisboa, Portugal; patricia@ipma.pt
8 Hellenic Centre for Marine Research, Anavyssos Attiki, 19013 Athens, Greece; kanast@hcmr.gr (A.A.); chryssi@hcmr.gr (C.M.)
9 MARBEC, University Montpellier, CNRS, Ifremer, IRD, 34200 Sète, France; Angelique.Jadaud@ifremer.fr
10 Agrocampus Ouest, UMR 985 ESE Ecologie et santé des écosystèmes, 35042 Rennes, France; marine_randon@sfu.ca
11 CEFAS, Pakefield Road, Lowestoft, Suffolk NR33 0HT, UK; joanne.smith@cefas.co.uk
12 ILVO—Institute for Agricultural and Fisheries Research, Ankerstraat 1, 8400 Oostende, Belgium; Karen.bekaert@ilvo.vlaanderen.be
13 Laboratoire d'Océanologie et de Géosciences, Université Littoral Côte d'Opale, University of Lille, CNRS, UMR 8187, LOG, 62930 Wimereux, France; rachid.amara@univ-littoral.fr
14 IFREMER, Sciences et Technologies Halieutiques, CS 10070, 29280 Plouzané, France; Helene.De.Pontual@ifremer.fr
15 MARBEC, University of Montpellier, IFREMER, CNRS, IRD, 34000 Montpellier, France; bruno.ernande@ifremer.fr
16 Evolution and Ecology Program, International Institute for Applied Systems Analysis (IIASA), Schlossplatz 1, A-2361 Laxenburg, Austria
* Correspondence: kelig.mahe@ifremer.fr; Tel.: +33-321-995-602

**Abstract:** The otolith, found in both inner ears of bony fish, has mainly been used to estimate fish age. Another application that has been developing significantly in recent years, however, is the use of otolith shape as a tool for stock identification. Often, studies have directly used the shape asymmetry between the right and left otoliths. We tested the magnitude of directional asymmetry between the sagittal otoliths (left vs. right) of 2991 individuals according to their catch locations, and we selected species to evaluate whether directional asymmetry may itself be a tool to evaluate stock boundaries. Elliptical Fourier descriptors were used to describe the otolith shape. We used a flatfish, the common sole (*Solea solea*, $n = 2431$), from the eastern English Channel and the southern North Sea as well as a roundfish, the bogue (*Boops boops*, $n = 560$), from the Mediterranean Sea. Both species showed significant levels of directional asymmetry between the testing locations. The bogue otoliths showed significant asymmetry for only 5 out of 11 locations, with substantial separation between two large areas: the Algerian coast and the western part of the Italian coast. The sole otoliths showed significant asymmetry in the shape analysis (3.84–6.57%), suggesting a substantial separation between two large areas: the English and French parts of the English Channel and the southern North Sea. Consequently, directional bilateral asymmetry in otolith shape is a potential new method for stock identification.



**Citation:** Mahé, K.; MacKenzie, K.; Ider, D.; Massaro, A.; Hamed, O.; Jurado-Ruzafa, A.; Gonçalves, P.; Anastasopoulou, A.; Jadaud, A.; Mytilineou, C.; et al. Directional Bilateral Asymmetry in Fish Otolith: A Potential Tool to Evaluate Stock Boundaries? *Symmetry* **2021**, *13*, 987. https://doi.org/10.3390/sym13060987

Academic Editor: Giorgio Vallortigara

Received: 15 April 2021
Accepted: 25 May 2021
Published: 1 June 2021

**Keywords:** otolith shape; side effect; Fourier descriptors; stock identification; Mediterranean Sea; Atlantic Ocean; common sole; bogue

## 1. Introduction

Otoliths are calcified structures, located in the inner ear cavity (left and right) of all teleost fish, that aid in hearing [1–3]. Otoliths show incremental structures with periodicity as they grow throughout the life of the fish and, unlike scales and bones, are metabolically inert (i.e., once deposited, otolith material is unlikely to be resorbed or altered) [4]. Consequently, otoliths have been primarily used as a tool for age determination in many fish species, thanks to the ability to track growth periodicity, from daily to annual growth increments. Moreover, otolith shape remains unaffected by short-term changes in fish condition [5] or environmental variation [1]. Accordingly, otolith shape has been used as a tool to identify species, reconstruct the composition of predator diet (fishes, seabirds, seals, etc.), and discriminate between fish stocks. Since Campana and Casselman in 1993 [5], many fishery scientists have developed this type of analysis for stock discrimination studies as a basis for understanding fish population dynamics and achieving reliable assessments for fishery management [6]. Several descriptors have been used to outline the external contour of otoliths: univariate descriptors (e.g., shape factors [7], geometric morphometric analyses [8–10], wavelet functions [11,12], growth markers [13], and the geodesic method [13]). However, elliptical Fourier analysis (EFA) remains the most widely used and robust method to describe otolith shape. As a result, 91 papers on the identification of marine fish populations or stock structure using otolith shape were published between 1993 and 2017.

The otolith shape of a fish depends on its genotype, the influence of environmental factors during its life (both biotic and abiotic), and on its stage of development (fish size, age, sex, and sexual maturation) [14–26]. Our review of the 91 published papers on marine fish stock identification based on otolith shape showed that only 20 of them estimated the asymmetry of both the right and the left otoliths (data from Web of Science with keywords "otolith" and "shape"; each publication was verified). Among 18 tested species, only 50% showed significant asymmetry of shape between otoliths.

In general, patterns of asymmetry in fish otoliths are classified into three types of asymmetries (Figure 1). Fluctuating asymmetry is the result of random deviations from perfect bilateral symmetry [27,28] and is usually associated with stress and/or environmental heterogeneity [27–30]. Lemberget and McCormick [28] suggested that fluctuating asymmetry could be considered as a sensitive indicator of fish health and directly affect fish performance because otoliths are essential to balance and hearing. Antisymmetry occurs when there is a systematic but alternating deviation towards one side or the other in the population, thus generating a bimodal distribution with a mean of 0 in its extreme form. Asymmetry that consistently favours one side across an individual group is referred to as directional asymmetry. Directional asymmetry characterizes the consistently greater development of one side of the inner ear among individuals in a population. In this context, the objectives of the present study were to explore (1) if otolith directional asymmetry shape is observable within the species and (2) if there was spatial variation within the study area. Our study species were the common sole (*Solea solea*, Linnaeus, 1758) and the bogue (*Boops boops*, Linnaeus, 1758). The common sole is a flatfish species (*Soleidae*) of large economic interest and is highly exploited in the Mediterranean Sea and the eastern Atlantic Ocean from Senegal to Norway, especially in the North Sea and the English Channel. This species lives on fine sand and muddy substrates between 0 and 150 m in depth. In the English Channel, reproduction takes place between February and June, with a peak from April to May, mainly in the coastal areas of the Dover Strait and larger bays [31]. The bogue is a common roundfish species (*Sparidae*) of the northeast Atlantic Ocean and the Mediterranean Sea. The bogue is a gregarious, demersal species found at depths between

0 and 350 m over a variety of substrates. In the Mediterranean Sea, it is one of the most abundant fish species [32].

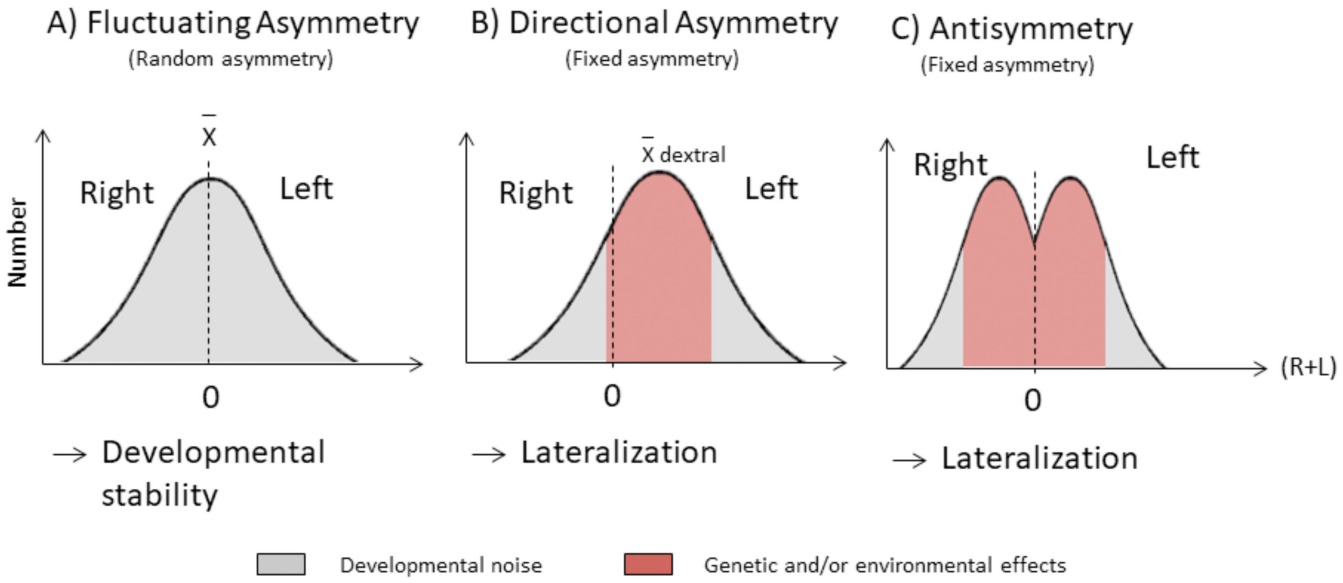


**Figure 1.** Categories of asymmetry: (**A**) fluctuating asymmetry represented by minor, non-directional deviations from perfect symmetry limited by the canalization process and the result of developmental noise; (**B**) directional asymmetry or lateralization process fixed on the same side, dependent on genotype and the influence of environmental (biotic and abiotic) factors throughout life; (**C**) antisymmetry or lateralization process fixed on the side, which varies randomly among individuals.

The aim of this study was to investigate whether the spatial variation of directional bilateral asymmetry in fish otoliths could be used as a potential tool to discriminate between stocks of fish as well as otolith shape.

## 2. Materials and Methods

### *2.1. Sample Collection*

A total of 2991 pairs of sagittal otoliths (left and right) were extracted from bogues ($n$ = 560) with a size range of 13 to 26 cm total length (TL) (18.38 ± 2.63 cm) and common soles ($n$ = 2431) with a size range of 9 to 34 cm TL (27.43 ± 9.62 cm). Fishes were collected from 17 different locations (Figure 2 and Table 1).

Bogue samples were collected from the Canary Islands to the Aegean Sea between 2013 and 2016, and common sole samples were collected from the western English Channel to the southern North Sea during 2017. Sampling was supported by 8 research institutes (Institut Français de Recherche pour l'Exploitation de la Mer (IFREMER), France; Centre for Environment, Fisheries and Aquaculture Science (CEFAS), UK; Institute for agricultural and fisheries research (ILVO), Belgium; Université Abderrahmane Mira, Algeria; APLYSIA institute, Italy; University of Tunis, Tunisia; Instituto Español de Oceanografía (IEO), Spain; and Hellenic Centre for Marine Research (HCMR), Greece) during four international surveys (Beam Trawl Survey (BTS), International Bottom Trawl Survey (IBTS), Channel Ground Fish Survey (CGFS), and International Bottom Trawl Survey in the Mediterranean Sea (MEDITS)). Samples were collected onboard fishing vessels and from fish markets. The age range of fish sampled was limited from 2 to 5 years to limit the bias of age on the otolith shape. Moreover, the macroscopic maturity stage was identified systematically to use only individuals beyond stage I (juvenile).

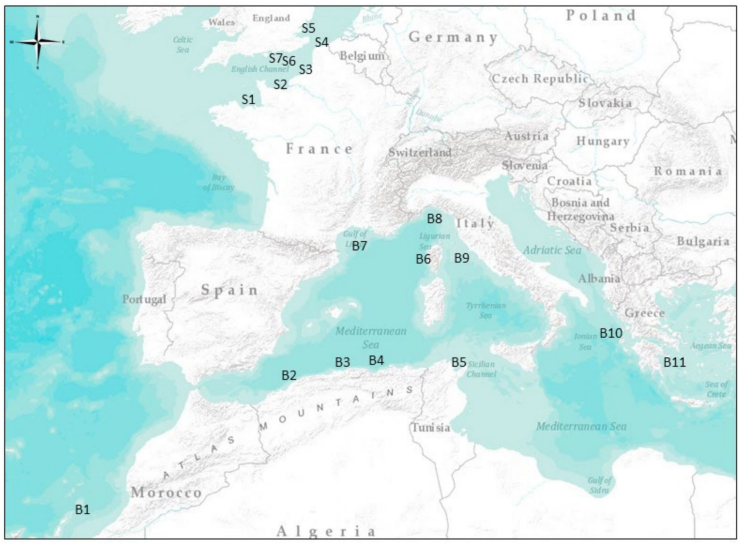


**Figure 2.** Map of sampling locations by species. *Boops boops* samplings were B1: Tenerife Island, B2: Gulf of Oran, B3: Gulf of Bejaia, B4: Gulf of Annaba, B5: Gulf of Tunis, B6: Corsica Island, B7: Gulf of Lion, B8: Ligurian Sea, B9: Tyrrhenian Sea, B10: Ionian Sea, and B11: Aegean Sea. *Solea solea* samplings were S1: Mont Saint Michel Bay, S2: Bay of Seine, S3: Bay of Somme, S4: French coast of the North Sea, S5: Thames Estuary, S6: central area of the eastern English Channel, and S7: English coast of the eastern English Channel.

**Table 1.** Fish number sampled by species and geographical area. Total length characteristics (mean ± SD) are given for each sample.

| Species | Geographical Area | | Number | Total Length (cm) | | | Sampling Period |
|---|---|---|---|---|---|---|---|
| | | | | Mean±SE | Minimum | Maximum | |
| *Boops boops* | B1 | Tenerife Island | 67 | 19.00 ± 0.93 | 18 | 20 | 11/2016 |
| | B2 | Gulf of Annaba | 40 | 19.12 ± 4.52 | 15 | 26 | 2/2013 to 12/2013 |
| | B3 | Gulf of Bejaia | 92 | 15.06 ± 1.70 | 11 | 19 | 1/2014 to 3/2014 |
| | B4 | Gulf of Oran | 47 | 15.50 ± 0.71 | 15 | 16 | 4/2015 |
| | B5 | Gulf of Tunis | 48 | 18.50 ± 1.02 | 17 | 21 | 7/2016 |
| | B6 | Corsica Island | 41 | 18.50 ± 1.91 | 16 | 20 | 6/2016 |
| | B7 | Gulf of Lion | 54 | 21.00 ± 4.69 | 15 | 25 | 6/2016 |
| | B8 | Ligurian Sea | 50 | 19.00 ± 1.74 | 17 | 23 | 6/2015 to 8/2015 |
| | B9 | Tyrrhenian Sea | 59 | 18.82 ± 2.07 | 16 | 21 | 6/2015 to 8/2015 |
| | B10 | Ionian Sea | 35 | 16.80 ± 2.86 | 15 | 23 | 9/2015 to 10/2015 |
| | B11 | Aegean Sea | 27 | 20.75 ± 0.71 | 17 | 22 | 9/2015 to 10/2015 |
| *Solea solea* | S1 | Mont Saint Michel Bay | 476 | 29.04 ± 8.21 | 16 | 39 | 4/2017 to 5/2017 |
| | S2 | Bay of Seine | 251 | 19.83 ± 7.75 | 15 | 27 | 4/2017 to 5/2017 |
| | S3 | Bay of Somme | 581 | 27.38 ± 4.60 | 24 | 34 | 4/2017 to 5/2017 |
| | S4 | French coast of the North Sea | 402 | 30.33 ± 2.50 | 26 | 34 | 4/2017 to 5/2017 |
| | S5 | Thames estuary | 297 | 28.71 ± 5.75 | 27 | 36 | 4/2017 to 5/2017 |
| | S6 | Central area of the eastern English Channel | 125 | 22.63 ± 7.04 | 18 | 26 | 4/2017 to 5/2017 |
| | S7 | English coast of the eastern English Channel | 299 | 29.04 ± 2.02 | 16 | 40 | 4/2017 to 5/2017 |

### *2.2. Otolith Shape Analysis*

A calibrated high-resolution image (3200 dpi) of the proximal face of the whole left and right sagittal otolith was obtained using a scanner with reflected light. Within this process, a fixed single magnification was used to ensure as high a resolution as possible.

Images were processed using the image analysis system TNPC (Digital processing for calcified structures, version 7) with the *sulcus acusticus* facing up. In order to compare left and right otolith shapes, mirror images of left otoliths were used.

An elliptic Fourier analysis (e.g., [33]) was carried out on each otolith contour delineated and extracted after image binarization. All EFDs were obtained using TNPC 7 software. For each otolith, the first 99 elliptical Fourier harmonics (H) were extracted and normalised with respect to the first harmonic and were thus invariant to otolith size, rotation, and starting point of contour description [34]. To determine the number of harmonics required to reconstruct the otolith outline, the cumulated Fourier power (F) was calculated for each individual otolith as a measure of the precision of contour reconstruction obtained with $n_k$ harmonics (i.e., the proportion of variance in contour coordinates accounted for by the $n_k$ harmonics):

$$F_{(n_k)} = \sum_{i=1}^{n_k} \frac{{A_i}^2 + {B_i}^2 + {C_i}^2 + {D_i}^2}{2} \quad (1)$$

where *Ai*, *Bi*, *Ci*, and *Di* are the coefficients of the $H_i$ harmonic. $F(n_k)$ and $n_k$ were calculated for each individual otolith k in order to ensure that each individual otolith in the sample was reconstructed with a precision of 99.99% [33]. The maximum number of harmonics $n = \max(n_k)$ across all otoliths was then used to reconstruct each individual otolith of the sample.

### *2.3. Statistical Analyses*

Asymmetry between left and right otolith shape was analysed as the effect of inner ear location (side, hereafter) on otolith shape. First, principal components analysis (PCA) was applied to a matrix of selected EFDs (EFDs as columns and individual otoliths as lines) of otolith contours [35], and a subset of the resulting principal components (PCs) was selected as otolith shape descriptors according to the broken stick model [36]. The matrix of selected PCs is referred to as 'shape matrix' hereafter. This procedure allowed us to decrease the number of variables used to describe otolith shape variability while ensuring that the main sources of shape variation were retained, and to avoid co-linearity between shape descriptors [35]. Second, partial redundancy analysis (pRDA) by species was performed on the shape matrix, using the side (left/right) as the potentially influential variable and the individual as the conditioning variable. This type of analysis was carried out for all individuals and then separately for each sampling location. pRDA is an extension of multiple regression to multivariate response data and an extension of PCA [36], combined with permutation tests (marginal effect, type II [37]) on the selected PCs matrix. To visualise differences in otolith shape between the right and left sides, an average otolith shape of each side group was rebuilt based on EFDs of the averaged shape. To evaluate DA amplitude, average left and right shapes were rebuilt based on EFDs averaged for each side at the level of all individuals and for each sampled location. DA amplitude was then computed as the percentage of non-overlapping surface between the reconstructed right and left otolith average shapes relative to the total area they covered after superposition.

Statistical analyses were performed in R [38] with 'Vegan' [39], 'SP' [40], 'RGEOS' [40], and 'MASS' [41] packages.

## 3. Results

Among the 99 Fourier harmonics extracted to describe individual otolith contours, the first 26 harmonics for bogue and the first 28 harmonics for common sole explained at least 99.99% of the variation in the otolith contour of each individual and were used for further analysis. After PCA on the elliptic Fourier descriptors (EFDs), only the first six PCs for both species were kept for the shape matrix, according to the broken-stick model. The pRDA performed on data across all sampling sites detected a significant directional asymmetry between left and right otolith shape ($p = 0.018$ for bogue and $p = 0.005$ for the common sole). The amplitudes of directional asymmetry across all sampling sites, measured as the percentage of non-overlapping surface between the right and left otolith shape, were on

average 2.77% for the bogue and 5.27% for the common sole (Figure 3). These two mean values showed significant directional asymmetry for the bogue and common sole.

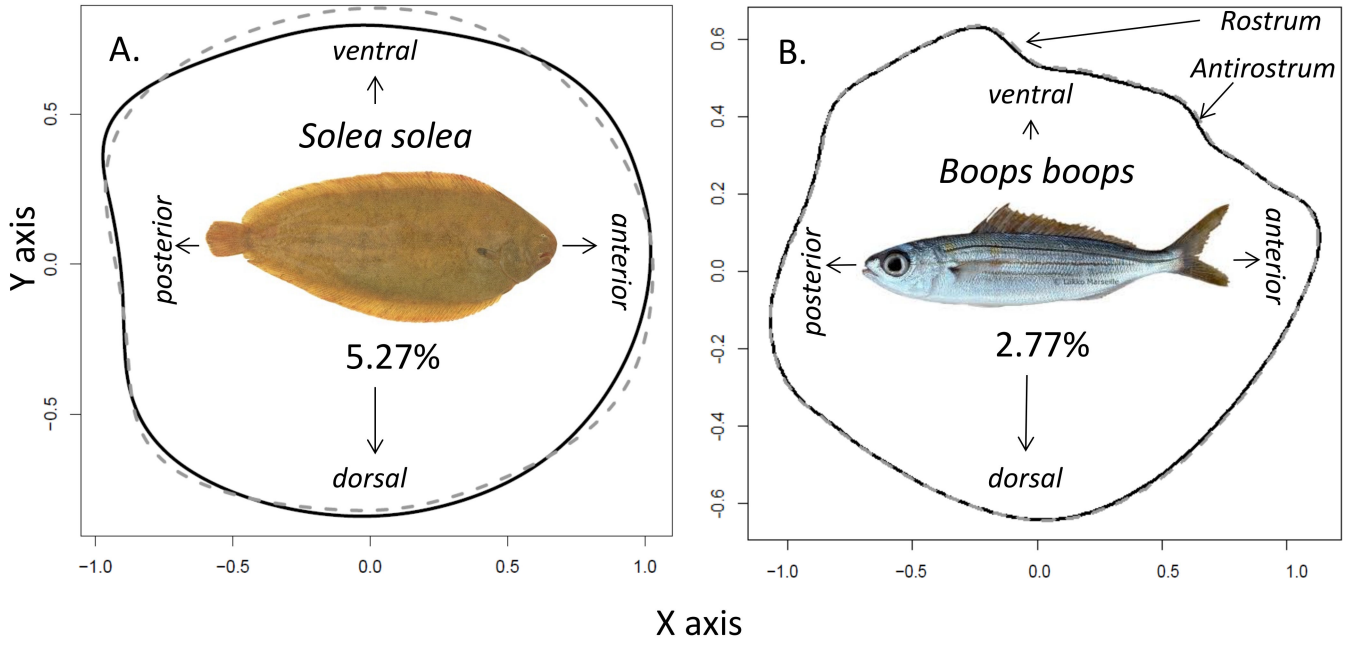


**Figure 3.** Differences among otolith mean shapes from the left (grey dotted line) and the right (black line) otolith. (**A**): *S. solea*; (**B**): *B. boops*.

In *B. boops*, only 5 out of 11 locations showed significant directional bilateral asymmetry, and these locations were in only two sectors: the Algerian coast (B2: Gulf of Oran, B3: Gulf of Bejaia, and B4: Gulf of Annaba) and the western part of the Italian coast (B8: Ligurian Sea and B9: Tyrrhenian Sea) (Figure 4). The main shape difference between left and right otoliths was located between the *rostrum* and the *antirostrum*. The right otolith was larger than the left otolith in the Ligurian and Tyrrhenian Seas, and this phenomenon was reversed in the Gulfs of Oran, Bejaia, and Annaba.

The mean level of bilateral asymmetry was higher in *S. solea* (5.27%) than in *B. boops* (2.77%) individuals. Moreover, all locations showed significant bilateral asymmetry on the same side, which characterized the directional asymmetry ($p < 0.05$ in pRDA for each location). The ventral part of the common sole otolith was the main area that showed asymmetry, with the left otolith consistently larger than the right. The asymmetry values varied in amplitude between 3.84% and 6.57%, depending on the sampling site (Figure 5). These mean values of asymmetries could be separated into two large areas: the English part of the studied area (Thames Estuary, central area of the eastern English Channel, and English coast of the eastern English Channel), with asymmetry values of 3.84% to 4.72%, and the French part of the studied area (Mont Saint Michel Bay, Bay of Seine, Bay of Somme, and the French coast of the North Sea), with values of 5.76% to 6.57% (Figure 5). The level of directional bilateral asymmetry between both parts of the eastern English Channel was significantly different ($p < 0.05$).

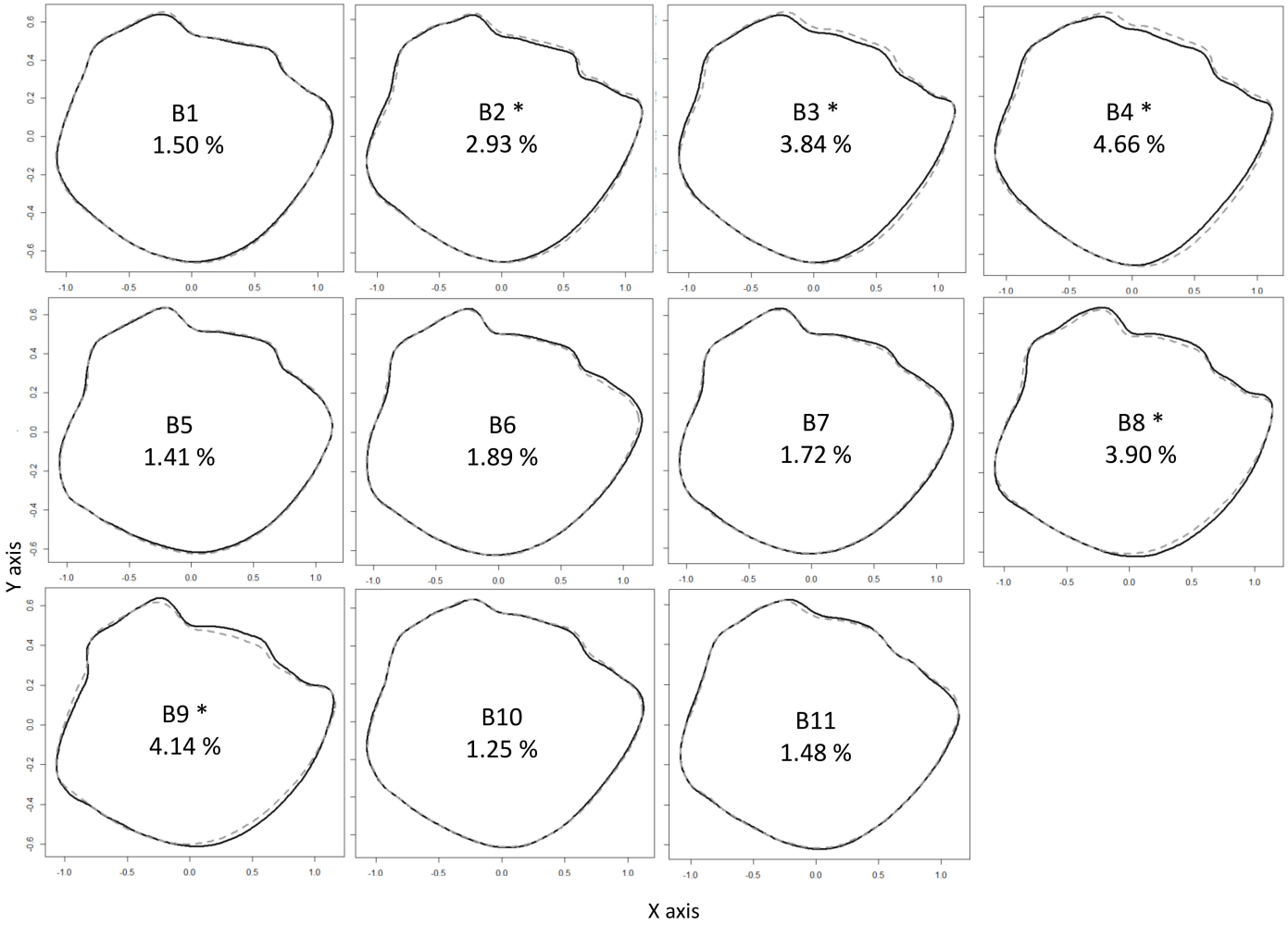


**Figure 4.** Differences between right (black line) and left (grey dotted line) otolith shape of *Boops boops* by each geographical location with the percentage of directional asymmetry (* = significant asymmetry). B1: Tenerife Island; B2: Gulf of Oran, B3: Gulf of Bejaia, B4: Gulf of Annaba, B5: Gulf of Tunis, B6: Corsica Island, B7: Gulf of Lion, B8: Ligurian Sea, B9: Tyrrhenian Sea, B10: Ionian Sea, B11: Aegean Sea.

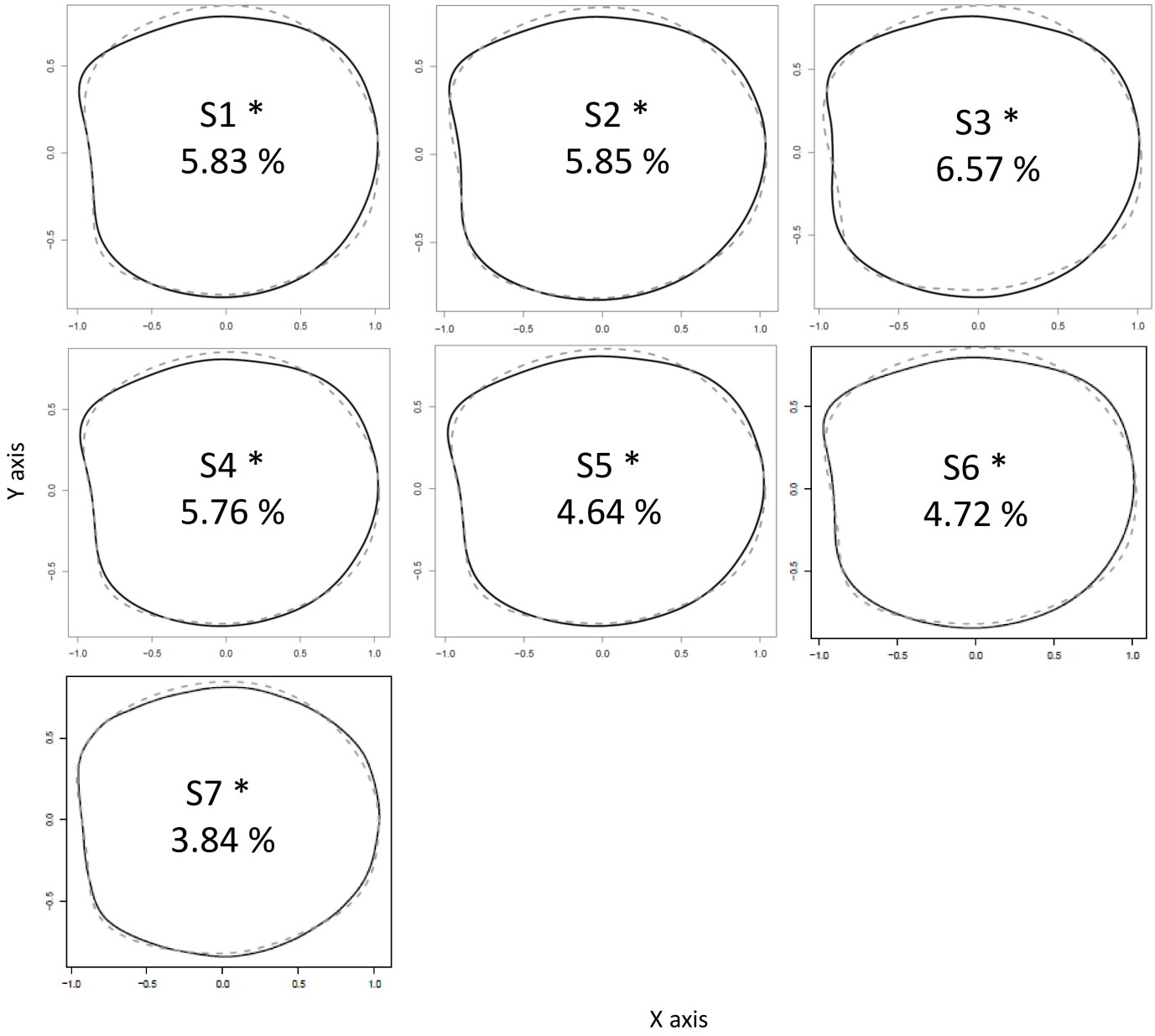


**Figure 5.** Differences between right (black line) and left (grey dotted line) otolith shape of *Solea solea* by each geographical location with the percentage of directional asymmetry (* = significant asymmetry). S1: Mont Saint Michel Bay, S2: Bay of Seine, S3: Bay of Somme, S4: French coast of the North Sea, S5: Thames Estuary, S6: central area of the eastern English Channel, S7: English coast of the eastern English Channel.

## 4. Discussion

Fish otolith shape is frequently used to discriminate between stock units within a species as a consequence of a number of factors, such as abiotic environmental parameters (e.g., temperature and salinity), biotic parameters (e.g., prey availability), and genetics [5,17,19,20,25,26,32]. Other ontogenetic factors, such as fish length [5,22,42,43], age [44], year class [5,7,45,46], sexual maturity [5,19], and sexual dimorphism [5,45] can also modify the otolith shape. However, the potential intra-individual factor between the right and left inner otolith as a source of variation in otolith shape has been very understudied. In biology, symmetry in bilaterally symmetrical organisms, including vertebrates, is so consistent as to be considered standard, and it is maintained by homeostatic processes [47]. However, numerous studies have documented a consistent asymmetry in human upper limb bones, with right side elements typically being larger, while lower limb bones tend to be more

symmetric [48]. Humans preferentially use the right upper limb, and many skeletal studies have argued that lateralized behaviours among humans lead to differences in bone size and shape between sides, especially for the upper limbs [49]. For the otolith shape, fluctuating asymmetry, defined as the random deviations from perfect symmetry between the left and right otoliths, has been reported for some species of both roundfish and flatfish [28,50–52]. Directional asymmetry has been measured for 18 fish species. Symmetry between the left and right otoliths, showing the two strictly similar parts of the vestibular system, has been observed in *Gadus morhua* [19,53], *Coryphaena hippurus* [54], *Xiphias gladius* [55], *Scomber scombrus* [14], *Melanogrammus aeglefinus* [56], *Mullus barbatus* [56], *Clupea harengus* [56], and *Lutjanus kasmira* [55]. Conversely, otolith directional asymmetry, showing lateralization, has been observed for the roundfish *Liza ramada* [57], *Diplodus annularis* [58], *Scomberomorus niphonius* [59], and *Merlangius merlangus* [56] as well as for the flatfish *Solea solea* [22,56], *Pleuronectes platessa* [56], *Limanda limanda* [56], and *Lepidorhombus whiffiagonis* [56]. This study corroborated the results observed in the otoliths of common sole, and identified otolith asymmetry in bogue. Directional bilateral asymmetry or antisymmetry in fish otoliths could be a result of differences in otolith biomineralisation between the left and right inner ears [56]. This asymmetry is an indicator of possible dysfunction, considering vestibular sensing [60]. Otolith directional asymmetry affects the acoustic functionality (sensitivity, temporal processing, and sound localization) [51,52] and kinetic swimming of fish (aberrant movement pattern or static space sickness) [60–63]. As in a previous study [56], our results showed that the observed level of otolith asymmetry in flatfish is higher than that in roundfish. For flatfish, the metamorphosis mechanism is an important source of shape asymmetry between the right and left otoliths because it causes a unique asymmetric body shape and lateralized behaviour due to adaptation to a bottom-living lifestyle, in addition to affecting the otolith shape of fish. In addition to the metamorphosis mechanism, other factors related to ontogeny (such as sexual maturity) could have potential effects on the level of directional bilateral asymmetry.

Otolith asymmetry could change during the life of a flatfish, especially after cranial deformation and the migration of one eye to the other side, caused by cell proliferation in suborbital tissue [64]. This lateralization process induces a difference in otolith biomineralisation (carbonate accretion rates), with the blind side generally growing faster in length and weight than the other side [56,65–67]. Gravity is probably also a source of otolith asymmetry in flatfish [61]. *Solea solea* is a dextral species (right-eyed flatfish) with the right inner ear above the left inner ear, and the left otolith is larger than the right otolith. Consequently, this study corroborated that the blind side was the location of the widest otolith for flatfish [22,56]. In conclusion, if directional asymmetry is observed more frequently in flatfish than roundfish species, there might be environmental patterns other than gravity to explain the degree of otolith shape asymmetry in fish species.

No study has previously examined the fluctuations of directional bilateral asymmetry in fish otoliths according to geographic origin. The canalization process is defined as the tendency of a specific genotype to follow the same phenotypic trajectory under varied developmental and environmental influences (developmental stability), and it limits potential directional asymmetry. One study showed that the magnitude of asymmetry between scallop (Bivalvia: Pectinidae) valve shape could be linked to the type of ecomorph and, therefore, a difference in environmental pressures [68]. For fish species, molecular investigations have suggested that mandibular asymmetry corresponds to genomic loci [69]. The morphological asymmetry of scale-eating cichlids in Lake Tanganyika has a genetic basis in two individual groups [70]. The directional asymmetry of dental formulae and arch shape identified the hybrids and the parental species of the clonal fish *Chrosomus eosneogaeus* [71]. This experimental study showed that left–right asymmetry in the dentition and shape of the pharyngeal arches reflected phenotypic plasticity. Similarly, a study on *Astyanax mexicanus* highlighted the use of directional asymmetry of osteocranial shape to identify specimens from the cavefish population in comparison with those from the surface population. This difference was not directly associated with eye loss, but with cave-adapted

fish [72]. Consequently, directional asymmetry concerning skeletal or calcified structures could be a genetic and/or phenotypic marker for studies on evolution, or it could be used as a tool to discriminate between populations.

For *Boops boops*, significant directional asymmetry associated with some geographical areas was observed, whereas no asymmetry was observed in other geographical areas. Fish in two large areas, the Algerian coast and the western part of the Italian coast, showed directional asymmetry, but these areas showed opposite differences between the left and the right otoliths. Consequently, this result suggests that the two specific individual groups are separated and that the Strait of Sicily is a mixed area influenced in the west by Atlantic Ocean currents and, conversely, in the east by the Levantine Intermediate Water current (LIW), which moves water masses from east to west [73]. There are no available data on the scale of the Mediterranean Sea on the stock distribution of *Boops boops*. On the Algerian coast, only one stock was identified for this area [74] as the result of asymmetry. For *Solea solea*, the otolith asymmetry values could be separated into two large areas: the English part and the French part of the English Channel and the southern North Sea. A previous study combined the life cycle stages, including (a) larval retention within spawning regions, (b) spatial segregation of juveniles inside separated coastal and estuarine nursery grounds, and (c) limited individual movement at the adult stages to identify three subpopulations of common sole in the eastern English Channel, with a separation between the English and the French parts [75]. Moreover, another study based on genotype and the otolith shape concluded that the structure of this species in the eastern English Channel was divided into several subunits, with noticeable isolation of the Seine River subunit [76]. The genetic and otolith shape approaches showed different discriminatory power. While these tools showed that the Seine River was isolated from the other parts of the eastern English Channel, the fish from the northeast and UK areas were not easily assigned according to the type of approach used (genetic or otolith shape). The discrimination difference explained by the otolith shape is related to a complex combination of genetic, ontogenetic, and environmental factors. As with otolith shape, the results of directional asymmetry identified two components in the fine-scale population structure of the common sole of the eastern English Channel. In conclusion, the directional bilateral asymmetry in fish otoliths confirms the conclusions of previous studies on stock discrimination using life history traits and otolith shape.

**Author Contributions:** K.M. (Kélig Mahé), R.A. (Rachid Amara), H.P., and B.E. designed the research; K.M. (Kélig Mahé), D.I., A.M. (Andrea Massaro), O.H., A.J.-R., P.G., A.A., A.J., C.M., M.R., Z.R., J.S. and K.B. realized the sampling; K.M. (Kélig Mahé), M.R., R.E., and A.M. (Alaia Morell) organized the image analysis; K.M. (Kélig Mahé) and B.E. performed the statistical analyses. All authors provided input for the results and discussion. K.M. (Kélig Mahé) wrote the paper. K.M. (Kirsteen MacKenzie) reviewed and edited the final English version. All authors provided critical comments and were involved in the writing of the manuscript. All authors have read and agreed to the published version of the manuscript.

**Funding:** This study was supported by the Data Collection Framework (DCF; EC Reg. 199/2008, 665/2008; Decisions 2008/949/EC and 2010/93/EU) and the French FFP project SMAC (Sole de Manche Est: Amélioration des Connaissances pour une meilleure gestion du stock).

**Data Availability Statement:** The data presented in this study are available upon request from the corresponding author.

**Acknowledgments:** We would like to express our gratitude to all people involved in the collection of samples required in this study. Thanks are expressed to all scientists and the crew for their help with sample collection.

**Conflicts of Interest:** The authors declare no conflict of interest.

## References


1. Campana, S.E. Chemistry and composition of fish otoliths: Pathways, mechanisms and applications. *Mar. Ecol. Prog. Ser.* **1999**, *188*, 263–297. [CrossRef]
2. Campana, S.E.; Thorrold, S.R. Otoliths, increments, and elements: Keys to a comprehensive understanding of fish populations? *Can. J. Fish. Aquat. Sci.* **2001**, *58*, 30–38. [CrossRef]
3. Panfili, J.; Pontual, H.de.; Troadec, H.; Wright, P.J. *Manual of Fish Sclerochronology*; Coédition Ifremer-IRD: Brest, France, 2002.
4. Casselman, J.M. Determination of age and growth. In *The Biology of Fish Growth*; Weatherley, A.H., Gill, H.S., Eds.; Academic Press: New York, NY, USA, 1987; pp. 209–242.
5. Campana, S.E.; Casselman, J.M. Stock discrimination using otolith shape analysis. *Can. J. Fish. Aquat. Sci.* **1993**, *50*, 1062–1083. [CrossRef]
6. Reiss, H.; Hoarau, G.; Dickey-Collas, M.; Wolff, W. Genetic population structure of marine fish: Mismatch between biological and fisheries management units. *Fish Fish.* **2009**, *10*, 361–395. [CrossRef]
7. Tuset, V.M. Use of otolith shape for stock identification of John's snapper, *Lutjanus johnii* (Pisces: Lutjanidae), from the Persian Gulf and the Oman Sea. *Fish. Res.* **2014**, *155*, 59–63.
8. Ponton, D. Is geometric morphometrics efficient for comparing otolith shape of different fish species? *J. Morphol.* **2006**, *267*, 750–757. [CrossRef]
9. Ramirez-Pérez, J.S.; Quiñónez-Velázquez, C.; García-Rodríguez, F.J.; Felix-Uraga, R.; Melo-Barrera, F.N. Using the shape of sagitta otoliths in the discrimination of phenotypic stocks in *Scomberomorus sierra* (Jordan and Starks, 1895). *Can. J. Fish. Aquat. Sci.* **2010**, *5*, 82–93.
10. Vergara-Solana, F.J.; García-Rodríguez, F.J.; De La Cruz-Agüero, J. Comparing body and otolith shape for stock discrimination of Pacific sardine, *Sardinops sagax* Jenyns, 1842. *J. Appl. Ichthyol.* **2013**, *29*, 1241–1246. [CrossRef]
11. Sadighzadeh, Z.; Valinassab, T.; Vosugi, G.; Motallebi, A.A.; Fatemi, M.R.; Lombarte, A.; Tuset, V.M.; Lozano, I.J.; Gonzalez, J.A.; Pertusa, J.F.; et al. Shape indices to identify regional differences in otolith morphology of comber, *Serranus cabrilla* (L., 1758). *J. Appl. Ichthyol.* **2003**, *19*, 88–93.
12. Parisi-Baradad, V.; Lombarte, A.; García-Ladona, E.; Cabestany, J.; Piera, J.; Chic, Ò. Otolith shape contour analysis using affine transformation invariant wavelet transforms and curvature scale space representation. *Mar. Freshw. Res.* **2005**, *56*, 795–804. [CrossRef]
13. Benzinou, A.; Carbini, S.; Nasreddine, K.; Elleboode, R.; Mahé, K. Discriminating stocks of striped red mullet (*Mullus surmuletus*) in the Northwest European seas using three automatic shape classification methods. *Fish. Res.* **2013**, *143*, 153–160. [CrossRef]
14. Castonguay, M.; Simard, P.; Gagnon, P. Usefulness of Fourier analysis of otolith shape for Atlantic mackerel (*Scomber scombrus*) stock discrimination. *Can. J. Fish. Aquat. Sci.* **1991**, *48*, 296–302. [CrossRef]
15. Lombarte, A.; Lleonart, J. Otolith size changes related with body growth, habitat depth and temperature. *Environ. Biol. Fishes* **1993**, *37*, 297–306. [CrossRef]
16. Begg, G.A.; Brown, R.W. Stock identification of haddock *Melanogrammus aeglefinus* on Georges Bank based on otolith shape analysis. *Trans. Am. Fish. Soc.* **2000**, *129*, 935–945. [CrossRef]
17. Cadrin, S.X.; Friedland, K.D. The utility of image processing techniques for morphometric analysis and stock identification. *Fish. Res.* **1999**, *43*, 129–139. [CrossRef]
18. Capoccioni, F.; Costa, C.; Aguzzi, J.; Menesatti, P.; Lombarte, A.; Ciccotti, E. Ontogenetic and environmental effects on otolith shape variability in three Mediterranean European eel (*Anguilla anguilla*, L.) populations. *J. Exp. Mar. Biol. Ecol.* **2011**, *397*, 1–7. [CrossRef]
19. Cardinale, M.; Doerin-Arjes, P.; Kastowsky, M.; Mosegaard, H. Effects of sex, stock, and environment on the shape of known-age Atlantic cod (*Gadus morhua*) otoliths. *Can. J. Fish. Aquat. Sci.* **2004**, *61*, 158–167. [CrossRef]
20. Gagliano, M.; McCormick, M.I. Feeding history influences otolith shape in tropical fish. *Mar. Ecol. Prog. Ser.* **2004**, *278*, 291–296. [CrossRef]
21. Hüssy, K. Otolith shape in juvenile cod (*Gadus morhua*): Ontogenetic and environmental effects. *J. Exp. Mar. Biol. Ecol.* **2008**, *364*, 35–41. [CrossRef]
22. Mérigot, B.; Letourneur, Y.; Lecomte-Finiger, R. Characterization of local populations of the common sole *Solea solea* (Pisces, Soleidae) in the NW Mediterranean through otolith morphometrics and shape analysis. *Mar. Biol.* **2007**, *151*, 997–1008. [CrossRef]
23. Mille, T.; Mahé, K.; Cachera, M.; Villanueva, C.M.; De Pontual, H.; Ernande, B. Diet is correlated with otolith shape in marine fish. *Mar. Ecol. Prog. Ser.* **2016**, *555*, 167–184. [CrossRef]
24. Monteiro, L.R.; Di Beneditto, A.P.M.; Guillermo, L.H.; Rivera, L.A. Allometric changes and shape differentiation of sagitta otoliths in sciaenid fishes. *Fish. Res.* **2005**, *74*, 288–299. [CrossRef]
25. Swan, S.C.; Geffen, A.J.; Morales-Nin, B.; Gordon, J.D.M.; Shimmield, T.; Sawyer, T.; Massutí, E. Otolith chemistry: An aid to stock separation of *Helicolenus dactylopterus* (bluemouth) and *Merluccius merluccius* (European hake) in the Northeast Atlantic and Mediterranean. *ICES J. Mar. Sci.* **2006**, *63*, 504–513. [CrossRef]
26. Vignon, M.; Morat, F. Environmental and genetic determinant of otolith shape revealed by a non-indigenous tropical fish. *Mar. Ecol. Prog. Ser.* **2010**, *411*, 231–241. [CrossRef]
27. Díaz-Gil, C.; Palmer, M.; Catalán, I.A.; Alós, J.; Fuiman, L.A.; García, E.; del Mar Gil, M.; Grau, A.; Kang, A.; Maneja, R.H.; et al. Otolith fluctuating asymmetry: A misconception of its biological relevance? *ICES J. Mar. Sci.* **2015**, *72*, 2079–2089. [CrossRef]

28. Lemberget, T.; Mccormick, M.I. Replenishment success linked to fluctuating asymmetry in larval fish. *Oecologia* **2009**, *159*, 83–93. [CrossRef]
29. Dowhower, J.F.; Blumer, L.S.; Lejeune, P.; Gaudin, P.; Marconato, A.; Bisazza, A. Otolith asymmetry in *cottus bairdi* and *cottus gobio*. *Pol. Arch. Hydrobiol.* **1990**, *37*, 209–220.
30. Green, A.A.; Mosaliganti, K.R.; Swinburne, I.A.; Obholzer, N.D.; Megason, S.G. Recovery of Shape and Size in a Developing Organ Pair. *Dev. Dyn.* **2017**, *246*, 451–465. [CrossRef]
31. Carpentier, A.; Coppin, F.; Curet, L.; Dauvin, J.C.; Delavenne, J.; Dewarumez, J.M.; Dupuis, L.; Foveau, A.; Garcia, C.; Gardel, L.; et al. *Atlas des Habitats des Ressources Marines de la Manche Orientale—CHARM II/Channel Habitat Atlas for Marine Resource Management—CHARM II. PROGRAMME INTERREG 3A*; IFREMER: Boulogne-sur-mer, France, 2009.
32. FAO. *The State of Mediterranean and Black Sea Fisheries 2016 (SoMFi 2016)*; Food and Agriculture Organization of the United Nations: Rome, Italy, 2016.
33. Lestrel, P.E. *Fourier Descriptors and Their Applications in Biology*; Cambridge University Press: Cambridge, UK, 2008.
34. Kuhl, F.; Giardina, C. Elliptic Fourier features of a closed contour. *Comput. Graph. Image Process.* **1982**, *18*, 236–258. [CrossRef]
35. Rohlf, F.J.; Archie, J.W. A Comparison of Fourier Methods for the Description of Wing Shape in Mosquitoes (Diptera: Culicidae). *Syst. Biol.* **1984**, *33*, 302–317. [CrossRef]
36. Legendre, P.; Legendre, L.F.J. *Numerical Ecology*, 2nd ed.; Elsevier Science: Amsterdam, The Netherlands, 1998.
37. Fox, J.; Weisberg, S. *An {R} Companion to Applied Regression*, 2nd ed.; SAGE Publications, Inc.: Thousand Oaks, CA, USA, 2011.
38. R Development Core Team. *R: A Language and Environment for Statistical Computing*; R Foundation for Statistical Computing: Vienna, Austria, 2016.
39. Oksanen, J.; Blanchet, F.G.; Kindt, R.; Legendre, P.; Minchin, P.R.; O'Hara, R.B.; Simpson, G.L.; Solymos, P.; Stevens, H.M.H.; Wagner, H. Vegan: Community Ecology Package. In *R Package Version 2.0–10*; R Foundation for Statistical Computing: Vienna, Austria, 2013.
40. Bivand, R.S.; Pebesma, E.; Gomez-Rubio, V. *Applied Spatial Data Analysis with R*, 2nd ed.; Springer: New York, NY, USA, 2013.
41. Venables, W.N.; Ripley, B.D. *Modern Applied Statistics with S*, 4th ed.; Springer: New York, NY, USA, 2002.
42. Torres, G.J.; Lombarte, A.; Morales-Nin, B. Sagittal otolith size and shape variability to identify geographical intraspecific differences in three species of genus *Merluccius*. *J. Mar. Biol. Assoc. UK* **2000**, *80*, 333–342. [CrossRef]
43. Smith, M.K. Regional differences in otolith morphology of the deep slope red snappers *Etelis carbunculus*. *Can. J. Fish. Aquat. Sci.* **1992**, *49*, 795–804. [CrossRef]
44. Bird, J.L.; Eppler, D.T.; Checkley, D.M. Comparisons of herring otoliths using Fourier series shape analysis. *Can. J. Fish. Aquat. Sci.* **1986**, *43*, 1228–1234. [CrossRef]
45. Bolles, K.L.; Begg, G.A. Distinction between silver hake (*Merluccius bilinearis*) stocks in U.S. waters of the northwest Atlantic using whole otolith morphometric. *Fish. Bull.* **2000**, *98*, 451–462.
46. Mapp, J.; Hunter, E.; Van Der Kooijc, J.; Songer, S.; Fisher, M. Otolith shape and size: The importance of age when determining indices for fish-stock separation. *Fish. Res.* **2017**, *190*, 43–52. [CrossRef]
47. Palmer, A.R. Animal asymmetry. *Curr. Biol.* **2009**, *19*, 473–477. [CrossRef] [PubMed]
48. Auerbach, B.M.; Ruff, C.B. Limb bone bilateral asymmetry: Variability and commonality among modern humans. *J. Hum. Evol.* **2006**, *50*, 203–218. [CrossRef]
49. Ambrose, S.H. Paleolithic technology and human evolution. *Science* **2001**, *291*, 1748–1753. [CrossRef]
50. Lychakov, D. Behavioral lateralization and otolith asymmetry. *J. Evol. Biochem. Physiol.* **2013**, *49*, 441–456. [CrossRef]
51. Lychakov, D.V.; Rebane, Y.T. Fish otolith mass asymmetry: Morphometry and influence on acoustic functionality. *Hear. Res.* **2005**, *201*, 55–69. [CrossRef]
52. Lychakov, D.V.; Rebane, Y.T.; Lombarte, A.; Demestre, M.; Fuiman, L.A. Saccular otolith mass asymmetry in adult flatfishes. *J. Fish Biol.* **2008**, *72*, 2579–2594. [CrossRef]
53. Petursdottir, G.; Begg, G.A.; Marteinsdottir, G. Discrimination between Icelandic cod (*Gadus morhua* L.) populations from adjacent spawning areas based on otolith growth and shape. *Fish. Res.* **2006**, *80*, 182–189. [CrossRef]
54. Duarte-Neto, P.; Lessa, R.; Stosic, B.; Morize, E. The use of sagittal otoliths in discriminating stocks of common dolphinfish (*Coryphaena hippurus*) off northeastern brazil using multishape descriptors. *ICES J. Mar. Sci.* **2008**, *65*, 1144–1152. [CrossRef]
55. Mahé, K.; Evano, H.; Mille, T.; Muths, D.; Bourjea, J. ; Otolith shape as a valuable tool to evaluate the stock structure of swordfish *Xiphias gladius* in the Indian Ocean. *Afr. J. Mar. Sci.* **2016**, *38*, 457–464. [CrossRef]
56. Mille, T.; Mahé, K.; Villanueva, C.M.; De Pontual, H.; Ernande, B. Sagittal otolith morphogenesis asymmetry in marine fishes. *J. Fish Biol.* **2015**, *87*, 646–663. [CrossRef]
57. Rebaya, M.; Ben Faleh, A.R.; Allaya, H.; Khedher, M.; Trojette, M.; Marsaoui, B.; Fatnassi, M.; Chalh, A.; Quignard, J.P.; Trabelsi, M. Otolith shape discrimination of *Liza ramada* (Actinopterygii: Mugiliformes: Mugilidae) from marine and estuarine populations in Tunisia. *Acta Ichthyol. Piscat.* **2017**, *47*, 13–21. [CrossRef]
58. Trojette, M.; Ben Faleh, A.; Fatnassi, M.; Marsaoui, B.; Mahouachi, N.H.; Chalh, A.; Quignard, J.-P.; Trabelsi, M. Stock discrimination of two insular populations of *Diplodus annularis* (Actinop-terygii: Perciformes: Sparidae) along the coast of Tunisia by analysis of otolith shape. *Acta Ichthyol. Piscat.* **2015**, *45*, 363–372. [CrossRef]

59. Zhang, C.; Ye, Z.; Li, Z.; Wan, R.; Ren, Y.; Dou, S. Population structure of Japanese Spanish mackerel *Scomberomorus niphonius* in the Bohai Sea, the Yellow Sea and the East China Sea: Evidence from random forests based on otolith features. *Fish. Sci.* **2016**, *82*, 251–256. [CrossRef]
60. Hilbig, R.; Knie, M.; Shcherbakov, D.; Anken, R.H. Analysis of Behaviour and Habituation of Fish Exposed to Diminished Gravity in Correlation to Inner Ear Stone Formation—A Sounding Rocket Experiment (TEXUS 45). In Proceedings of the 20th ESA Symposium on European Rocket and Balloon Programmes and Related Research, Hyere, France, 22–26 May 2011.
61. Anken, R.; Kappel, T.; Rahmann, H. Morphometry of fish inner ear otoliths after Development at 3g hypergravity. *Acta Oto-Laryngol.* **1998**, *118*, 534–539.
62. Beier, M.; Anken, R.; Rahmann, H. Susceptibility to abnormal (kinetotic) swimming in fish correlates with inner ear carbonic anhydrase-reactivity. *Neurosci. Lett.* **2002**, *335*, 17–20. [CrossRef]
63. Hilbig, R.; Anken, R.; Rahmann, H. On the origin of susceptibility to kinetotic swimming behaviour in fish: A parabolic aircraft flight study. *J. Vestib. Res.* **2003**, *12*, 185–189.
64. Bao, B.; Ke, Z.; Xing, J.; Peatman, E.; Liu, Z.; Xie, C.; Xu, B.; Gai, J.; Gong, X.; Yang, G.; et al. Proliferating cells in suborbital tissue drive eye migration in flatfish. *Dev. Biol.* **2011**, *351*, 200–207. [CrossRef]
65. Sogard, S.M. Interpretation of otolith microstructure in juvenile winter flounder (*Pseudopleuronectes americanus*): Ontogenetic development, daily increment validation, and somatic growth relationships. *Can. J. Fish. Aquat. Sci.* **1991**, *48*, 1862–1871. [CrossRef]
66. Helling, K.; Scherer, H.; Hausmann, S.; Clarke, A.H. Otolith mass asymmetries in the utricle and saccule of flatfish. *J. Vestib. Res.* **2005**, *15*, 59–64. [PubMed]
67. Fischer, A.J.; Thompson, B.A. The age and growth of southern flounder, *Paralichthys lethostigma*, from Louisiana estuarine and offshorewaters. *Bull. Mar. Sci.* **2004**, *75*, 63–77.
68. Sherratt, E.; Serb, J.M.; Adams, D.C. Rates of morphological evolution, asymmetry and morphological integration of shell shape in scallops. *BMC Evol. Biol.* **2017**, *17*, 248. [CrossRef]
69. Stewart, T.; Albertson, R.C. Evolution of a unique predatory feeding apparatus: Functional anatomy, development and a genetic locus for jaw laterality in Lake Tanganyika scale-eating cichlids. *BMC Biol.* **2010**, *8*, 8. [CrossRef]
70. Hata, H.; Yasugi, M.; Takeuchi, Y.; Takahashi, S.; Hori, M. Measuring and evaluating morphological asymmetry in fish: Distinct lateral dimorphism in the jaws of scale-eating cichlids. *Ecol. Evol.* **2013**, *3*, 4641–4647. [CrossRef]
71. Leung, C.; Duclos, K.K.; Grünbaum, T.; Cloutier, R.; Angers, B. Asymmetry in dentition and shape of pharyngeal arches in the clonal fish *Chrosomus eosneogaeus*: Phenotypic plasticity and developmental instability. *PLoS ONE* **2017**, *12*, e0174235. [CrossRef] [PubMed]
72. Powers, A.K.; Davis, E.M.; Kaplan, S.A.; Gross, J.B. Cranial asymmetry arises later in the life history of the blind Mexican cavefish, *Astyanax Mex*. *PLoS ONE* **2017**, *12*, e0177419. [CrossRef] [PubMed]
73. Skliris, N. Past, present and future patterns of the thermohaline circulation and characteristic water masses of the Mediterranean sea. In *The Mediterranean Sea—Its History and Present Challenges*; Goffredo, S., Dubinky, Z.D., Eds.; Springer: New York, NY, USA, 2014; pp. 29–48.
74. Ider, D.; Ramdane, Z.; Mahé, K.; Dufour, J.L.; Bacha, M.; Amara, R. Use of otolith shape analysis to discriminate stocks of *Boops boops* (L.) from the Algerian coast (southwestern part of the Mediterranean Sea). *Afr. J. Mar. Sci.* **2017**, *39*, 251–258. [CrossRef]
75. Archambault, B.; Rivot, E.; Savina, M.; Le Pape, O. Using a spatially structured life cycle model to assess the influence of multiple stressors on an exploited coastal-nursery-dependent population. *Estuar. Coast. Shelf Sci.* **2018**, *201*, 95–104. [CrossRef]
76. Randon, M.; Le Pape, O.; Ernande, B.; Mahé, K.; Volckaert, P.; Petit, E.J.; Lassalle, G.; LeBerre, T.; Réveillac, E. Complementarity and discriminatory power of genotype and otolith shape in describing the fine scale population structure of an exploited fish, the common sole of the Eastern English Channel. *PLoS ONE* **2020**, *15*, e0241429. [CrossRef] [PubMed]